# Poly(oxazoline) for the design of amphiphilic silicone coatings

Émilie Portier, Fabrice Azemar, Belkacem Tarek Benkhaled, Jean-François Bardeau, Fabienne Faÿ, Karine Réhel, Vincent Lapinte, Isabelle Linossier

# Poly(oxazoline) for the design of amphiphilic silicone coatings

Émilie Portier [a], Fabrice Azemar [a,*], Belkacem Tarek Benkhaled [b], Jean-François Bardeau [c], Fabienne Faÿ [a], Karine Réhel [a], Vincent Lapinte [b], Isabelle Linossier [a]

[a] Laboratoire de Biotechnologie et Chimie Marines, Univ. Bretagne-Sud, EA 3884, LBCM, IUEM, F-56100, Lorient, France
[b] ICGM, Univ Montpellier, CNRS, Montpellier, France
[c] Institut des Molécules et Matériaux du Mans UMR CNRS 6283, Faculté des Sciences / Le Mans Université, Avenue Olivier Messiaen, 72085, Le Mans Cedex 9, France

ABSTRACT

Fouling release coatings are known to be ecofriendly and to be a good alternative to the coatings containing biocides. To improve their efficiency and lifespan the incorporation of additives seems required. Amphiphilic system as PEG-silicone coatings have a lower impact on the environment. However, PEG oxidation in seawater impacts its lifespan. In this context, the development and incorporation of new hydrophilic additives offers great potentiel. The objective of this study is to design an amphiphilic fouling release coating containing poly(oxa- zoline) (POx) as additives. POx have similar physical properties as PEG and have already been used in biomedical applications.

POx with a trimethoxysilane end-group has been synthesized to be crosslinked in a RTV silicone coating. The impact of its incorporation in a PDMS coating has been evaluated on surface properties and on coating orga- nization. The results have been compared with a similar PEG-silicone coating. In addition, microbiologic assays have been carried out to evaluate the bacterial adhesion and the fouling properties of the coating. Two bio- medicals bacteria and a marine bacterium were used to confirm the interest of POx.

POx-silicone coating showed similar fouling efficiency against bacteria as PEG-silicone coating despite a bigger surface roughness and a lower compatibility with PDMS.

## 1. Introduction

*Staphylococcus aureus*, a gram + bacteria, and *Pseudomonas aeruginosa*, a gram – bacteria, are opportunistic pathogens causing both acute and chronic infections and are known as responsible for numerous hospital acquired nosocomial infections. Nowadays, the most frequent nosocomial infections are catheters-associated urinary tract infections, catheters-associated blood infections and pulmonary infections. This is due to the fact that microorganisms and in particular bacteria are able to adhere to biotic or abiotic surfaces [1]. With favourable conditions, they colonize the surfaces and develop biofilms. They are microbial sessile communities, attached to a substratum embedded in a secreted extracellular matrix [2,3]. These microbial communities exhibit and increase tolerance to both antimicrobial and disinfectant chemicals [4,5]. Similarly, marine biofilms, also named biofouling, have harmful economic and ecological impacts. They are responsible for corrosion of marine surfaces, an increase in fuel consumption of ships, and the release of toxic compounds. Ships are indeed protected by these antifouling coatings which contain biocide molecules which are released into the sea. Biofouling is also responsible for species-relocation and the widespread introduction and dissemination of invasive [6,7]. Seeing all the problemes mentioned above it seems urgent and important to develop new alternatives, especially new coatings which are ecofriendlier in order to inhibit the adhesion of microorganisms, in both medical and marine domains.

The development of fouling release coatings has been done with this aim in sight. Silicone coatings are widely used for their biocompatibility, low toxicity, ease of fabrication and use, as well as their low manufacturing costs [8]. To improve the efficiency of these kind of surfaces against biofouling, the incorporation of additives has been the subject of intensive research. The first category of additives used was silicone oil [9–11]. The formation of oil layer at the coating surface limits the fouling development and increases the efficiency of fouling release coatings. However, the non-toxicity of silicone oil is not yet clear for either aqueous environments or the human body. Various research works have shown that their uses can lead to damages to both macro and

* Corresponding author.
*E-mail address:* fabrice.azemar@univ-ubs.fr (F. Azemar).

https://doi.org/10.1016/j.porgcoat.2020.106116

microorganisms [12–14]. Another strategy is also to use hydrophilic polymers to obtain an amphiphilic coating [15]. This system is less toxic for the environment. Poly(ethylene glycol) and PEG derivatives are widely used to study both the effects of the surface chemistry and wetting ability on bacterial and proteins adsorptions [16,17]. Wu and Hjort have shown a significant reduction in nonspecific adsorption of proteins, whereas Camos Noguer et al. have studied the advantages of PEG-silicone coatings over conventional silicones against the prolifera- tion of diatoms [18].

The aim of this work is to study the potential of poly(oxazoline) (POx) as an additive for amphiphilic fouling release coating. The physicochemical properties of POx is similar to PEG in terms of viscosity, friction, diffusion, sedimentation, effective hydrodynamic diameter, hydrodynamic volume, or combinations of these [19]. In addition, POx has several advantages compared to PEG, the most important ones being that POx can be easily synthetized and need non-explosive monomer unlike PEG [20]. Nowadays, POxs are regarded as a PEG alternative in response to the overconsumption of PEG in cosmetic and biomedical fields [21]. The versatility of POx use comes from the variety of the R group substituting the monomer [22,23]. Chemical stability is another important parameter for coating performance and lifetime. Major metabolic pathways and (patho)physiological processes in many organisms, including humans, depend on, or are connected with oxidative modification or the degradation of molecules [24]. The pseudo-polypeptide structure of the poly(oxazoline) is more stable against the oxidation than PEG [20]. Furthermore, due to the large commercialisation of PEG in the biomedical field, Yang and Lai have shown the production of PEG antibodies [25].

In this study, a linear poly(2-methyl-2-oxazoline) homopolymer was used as additive in a silicone coating. The coating structure was characterized in terms of surface topography, additives incorporation and surface hydrophobicity to evaluate the impact of the additive into a silicone film. In addition, biological assays were done with three bacteria to measure the POx influence on their adhesion. All the results were compared with a silicone coating containing a linear PEG with the same molecular weight and with a silicone coating without any hydrophilic additive.

## 2. Experiment

### 2.1. Materials

Allylic alcohol, methyl tosylate, allylamine, diethyl ether, 6-mercaptohexanol, Darocur1173, 3-(triethoxysilyl)propyl isocyanate and dibutyl tin dilaurate (DBTDL), 2,2-dimethoxy-2-phenylacetophenone, PEG allyl terminated were purchased from Aldrich, (3-mercaptopropyl)trimethoxysilane was purchased from TCI and silicon matrix Dowsil 7091 was provided by Dow and used as received. Acetonitrile was dried and distilled according to standard procedures [26]. 2-Methyl-2-oxazoline (MOx) was dried, distilled from $CaH_2$ and stored under a dry nitrogen atmosphere.

### 2.2. Additives synthesis

#### 2.2.1. PEG functionalisation with a trimethoxysilane end-group

The crosslinkable PEG was prepared using thiol-ene reaction. PEG allyl terminated (10 g, 1 equivalent) was mixed with 2,2-dimethoxy-2-phenylacetophenone (0.233 g, 1 equivalent), (3-mercaptopropyl)trimethoxysilane (1.963 g, 1.2 equivalent) and finally dissolved in $CHCl_3$ (10 mL). The medium was placed under UV at 365 nm, and the thiol-ene reaction occurred over 2 h under reflux at room temperature. In order to avoid any crosslinking reaction with ambient air, the solvent was removed under vacuum (Fig. 1). The purified PEG was finally analyzed by $^1$H NMR spectroscopy. $^1$H NMR ($CDCl_3$, 60 MHz): 0.5–1.0 ppm ($SCH_2CH_2Si$), 1.5–2.0 ppm ($SCH_2CH_2Si$), 2.5 ppm ($SiOCH_3$), 3.3 ppm ($OCH_3$) and 3.7 ppm ($OCH_2CH_2O$).

#### 2.2.2. Synthesis of POx by cationic ring-opening polymerization (CROP) using allylamine: POx-allyl

2-Methyl-2-oxazoline (10 g, 30 equivalent) and methyl tosylate (0.875 g, 4.7 mmol) were dissolved in dry acetonitrile (4 M). The solution was vigorously stirred at 80 °C for a night. The reaction product was quenched by addition of an adequate amount of allylamine (5 equivalent). The flask was maintained for 24 h at 50 °C. After cooling, the polymer was isolated by slow precipitation from cold diethyl ether in 93% weight yield.

1H NMR (CDCl3) δ (ppm): 5.8 (m, 1H, CH), 5.2 (m, 2H, CH2), 3.9–3.2 (m, 4 nH, CH2 of POx), 3.8 (m, 2H, $CH_2$–CH = $CH_2$), 3.0 (m, 3H, terminal CH3), 2.3–1.8 (s, 3 nH, CH3 of POx).

#### 2.2.3. POx functionalization by thiol-ene coupling: POx-S OH

= POx-allyl (2 g, 1 mmol), 6-mercaptohexanol (0.67 g, 5 equiv. per C C) and Darocur1173 (0.082 g, 0.5 equiv.) were dissolved in DMF (10 mL). The reaction mixture was illuminated under 365 nm for 8 h. The reaction mixture was poured in a large excess of cold ethyl ether. The resulting polymer was isolated in 86% yield.

1 H NMR (CDCl3) δ (ppm): 3.9–3.3 (m, 4 nH+4, CH2 of POx and $CH_2$–OH, $CH_2$-S), 3.0 (m, 3H, terminal CH3), 2.4–1.8 (s, 3 nH, CH3 of POx), 1.2 (m, alkyl $CH_2$), 0.8 (m, alkyl $CH_2$).

#### 2.2.4. POx functionalization with a triethoxysilane end-group: POx-S-SiOEt

POx-S–OH (0.5 g, 2.5 mmol), 3-(triethoxysilyl)propyl isocyanate (0.0368 g, 1.1 equivalent) and DBTDL (0.063 mmol, 0.8 w%) were dissolved in acetonitrile (5 mL). The reaction mixture was stirred at room temperature for 72 h under a nitrogen atmosphere. The reaction mixture was poured in a large excess of cold ethyl ether.

1 H NMR (CDCl3) δ (ppm): 4.0–3.2 (m, 4 nH, CH2 of POx), 3.7 (q, 8H, SiO-$CH_2$–$CH_3$), 3.0 (m, 3H, terminal CH3), 2.4–1.8 (s, 3 nH, CH3 of POx), 1.2 (m, SiO–$CH_2$-$CH_3$ and alkyl $CH_2$), 0.8 (m, alkyl $CH_2$).

### 2.3. Coatings preparation

To evaluate the poly(oxazoline) influence on fouling release coatings, three coatings were prepared. A coating containing a commercial biomedical RTV (room temperature vulcanization) silicone matrix using as reference and two coatings with 10% by weight of hydrophilic additives (PEG and POx) in addition to the industrial silicone matrix. The same procedure was performed for each coating.

The silicone matrix and the additive were dissolved in THF (50% by weight). The mixture was introduced in a vial hermetically sealed and was agitated (180 rpm) at room temperature overnight. Then, the mixture was applied on a glass slide with a bar coater (500 µm). Finally, the silicone film was dried 48 h at room temperature to allow a complete crosslinking.

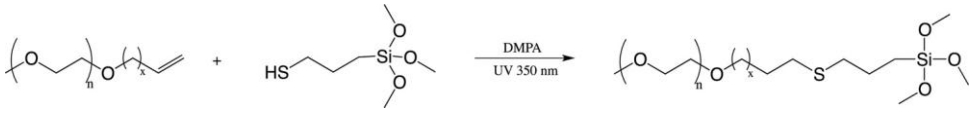


**Fig. 1.** Modification of the PEG additives by thiol-ene.

### 2.4. Coatings characterisation

A glass slide coated with a neat silicone matrix was used as reference to evaluate the impact of the hydrophilic additives on the physical and chemical properties of the modified samples. The silicone matrix used for this project is a commercial matrix containing some fillers to promote a good adhesion on the support. Moreover, a glass slide with PEG-silicone amphiphilic FRC was used to evaluate the interest of POx. PEG has been widely used as an additive for fouling release.

#### 2.4.1. Contact anglemeasurement

To determine the presence of the hydrophilic additives onto the surface of modified silicones, the contact angle kinetics of a 2 µL drop of water was measured during 180 s after contact between the drop and the film surface. Measurements were taken at room temperature with a contact angle system (Digidrop GBX) equipped with a syringe, a video camera, and an acquisition of angle measurements. The indicated values are an average of 15 measurements taken on different areas of three films.

#### 2.4.2. Scanning electron microscopy

The coated surface was observed with an electron microscope JEOL IT500 HR. The dried film was directly sputtered with carbon and the 1.9 kV beam energy was used to detect surface changes at the limit micro, nano-level (200 X of magnification).

#### 2.4.3. Optical profilometer

The 3D surface scans of the samples were undertaken using the confocal white light optical imaging S-NEOX profiler (Sensofar-Tech S. L., Barcelona, Spain). The 340× 284 $\mu m^2$ area were collected using a50 X DI Nikon objective (0.8 numerical aperture). The data were analyzed by MountainsMap®Imaging Topography software (8.0.9038 version, Digital Surf, France).

#### 2.4.4. Confocal Raman spectroscopy

The Raman measurements were performed at room temperature using a WITec Alpha 300R confocal Raman spectrometer (WITec GmbH, Ulm Germany) equipped with a 600 g $mm^{-1}$ grating and a Si-based charge-coupled device (CCD) front-illuminated camera (Andor, Oxford Instrument, Belfast, Ireland) with 1650 × 200 pixels cooled to - 60 °C in order to reduce thermal noise. Raman spectra were acquired in back-scattering under a microscope with a Zeiss EC Epiplan-Neofluar® 100× objective (numerical aperture of 0.9) focusing the 532 nm line of a Solid State Sapphire laser (Coherent INC., Santa Clara, USA). In order to chemically characterize the distribution of PEG and POx additive into the silicone matrix, a series of Raman spectra were recorded along a transverse section (depth analysis) and at the surface. For the depth analysis, each single Raman spectrum was systematically recorded 30 times with an integration time of 1 s (and a laser power at the sample of 30 mW) and averaged to improve the signal-to-noise ratio. The spectrometer being equipped with a motorized scanning stage, mapping areas were also performed. 3600 spectra were then recorded from a mapping 30 × 30 $\mu m^2$ area (2D map step size of around 0.5 µm) with a laser power at the sample of 30 mW and an integration times set at 0.5 s. The spectral analysis was performed using the WITec Project plus software (version 5.248, WITec GmbH, Germany).

### 2.5. Bacterial strains and growth conditions

Three bacterial strains were used for this study. *Staphylococcus aureus* CIP53154 (Methicilin-resistant-Staphylococcus aureus) and *Pseudomonas aeruginosa* (MPaO1, manoil lab Washington) were grown in Luria Bertani broth (10 $g.L^{-1}$ NaCl, 10 $g.L^{-1}$ Tryptone, 5 $g.L^{-1}$ yeast extract, pH 6.9), or agar (15 $g.L^{-1}$), at 37 °C.

The third strain was a marine bacterium, *Pseudoalteromonas* 5M6, isolated from the gulf of Morbihan, in France. This strain was grown in Zobell broth (4 $g.L^{-1}$ tryptone, 1 $g.L^{-1}$ yeast extract, 30 $g.L^{-1}$ sea salts), or agar (15 $g.L^{-1}$) at 20 °C. All the mediums were sterilized 20 min at 121 °C.

### 2.6. Biological assay

#### 2.6.1. Cytotoxicity assay

The cytotoxicity of PDMS, PDMS-PEG and PDMS-POX was estimated against *Pseudoalteromonas* 5M6, *S. aureus* and *P. aeruginosa.* These assays were performed using 24-well microtiter plates (reference). The neat PDMS and the modified silicone samples were spread at the bottom of wells and plates were UV-sterilized for 30 min. Bacteria were pre-cultured on LB agar or Zobell agar for 24 h. Then, bacteria were suspended in Zobell or LB medium to $1×10^6$ cfu and 1 mL was put down on wells. Plates were incubated 24 h, at 37 °C or 20 °C, under shacking (150 rpm) and optical density ($OD_{600\ nm}$) were measured. The experiment was repeated three times with similar results.

#### 2.6.2. Adhesion experiment

The aim of this experiment was to test and compare the adhesion strength of different micro-organisms on these surfaces. This investigation was performed using a sterilized flow cell system. Three channels flow-cells (1 ×40 4× mm; Biocentrum DTU, Denmark) were prepared with the surfaces. Each flow-cell was UV-sterilized for 30 min. Bacteria were pre-cultured for 24 h on LB or Zobell agar. *S. aureus* and *P. aeruginosa* were suspended in sterile physiological water (0.9 % NaCl) to $10^8$ cfu per mL. *Pseudoalteromonas* 5M6 was suspended in sterile artificial salted water (30 $g.L^{-1}$ sea salts), to 2.5 $10^8$ cfu per mL.

250 µL of suspensions were injected into each channel. The adhesion step was performed at room temperature, in static condition, for two hours. After this time laps, the flow (0.25 $mL.min^{-1}$; 6.16 mPa) was activated for one hour in order to remove planktonic bacteria. Planktonic cells were collected. In a last stage, the flow was increased (2.95 $mL.min^{-1}$) for 30 min to assess the adhesion strength of bacteria on the different surfaces. Detached bacteria were sampled.

For estimation of viable cell counts, serial 10 fold-dilutions were done and 100 µL of each dilution were plated on LB or Zobell agar. 10 µL aliquots taken from these dilutions were spotted on LB or Zobell plates. The number of CFU was determined after 24 h of incubation at 37 or 20 °C.

The experiment was repeated five times with similar results. Five independent experiments were performed, and each dilution was spread in triplicate. Data are expressed as mean+/- standard error of mean (SEM).

#### 2.6.3. Scanning electron microscope

*S. aureus* was precultured on LB agar for 24 h and suspended in sterile physiological water (0.9% NaCl) to $10^8$ cfu per mL. Pieces of the three surfaces were cut, UV-sterilized and put into small glass bottom containing bacterial suspension. After two hours of adhesion at room temperature, cells were fixed with 3% glutaraldehyde in phosphate buffer (0.1 M, pH 7.35), for 24 h at 4 °C. Surfaces were washed three times in phosphate buffer. Samples were dehydrated with ethanol solutions: three washes with 50% ethanol solution, three washes with 95% ethanol solution and three washes with absolute ethanol. The samples were dried by critical point drying using absolute ethanol and liquid carbon dioxide as the transition fluid (Tousimis – samdri PVT 3D). The dried surfaces were sputtered with gold and observed with Jeol IT500 HR (SED; 3 kV beam energy).

## 3. Results and discussion

### 3.1. Hydrophilic additives preparation

Poly(oxazoline) and poly(ethylene glycol) additives were synthesized and modified in order to obtain a hydrophilic polymer chain with a

trimethoxysilane end-group. The terminal moiety acts as reactive linker with silicone matrix to limit the additives release. $^1$H NMR spectroscopy was employed to check the chemical modification of POx and PEG and GPC to evaluate its integrity. The trimethoxysilane function can react with the atmosphere humidity and provides unwanted crosslinking of polymeric material preventing the reaction with the silicone matrix. The hydrophilic additives were conserved under nitrogen.

The synthesis of well-defined hydrophilic additives with a terminal crosslinking moiety was monitored by $^1$H NMR spectroscopy. The synthetic route for POx additives required three steps as illustrated in Fig. 2. First, POx was functionalized during the termination step of the cationic ring-opening polymerization (CROP) of 2-methyl-2-oxazoline by adding of allylamine. The occurrence of the allyl end-group was checked with the appearance of the characteristic signal of ethylenic protons at 6-5 ppm. The PEG and POx modification occurred by the same thiol-ene coupling between terminal allyl group of polymers and a reactant bearing a thiol moiety, (3-mercaptopropyl)trimethoxysilane for PEG and 6-mercaptohexanol for POx. As evidenced in Fig. 3, the disappearance of the allylic protons shows the thiol-ene reaction efficiency. A supplementary step of functionalization for POx was used with the conversion of the hydroxy end-group into urethane using 3-(triethoxysilyl)propyl isocyanate. For PEG, trimethoxysilane protons were detected in the region of 3.0–0.5 ppm while for POx, triethoxysilane protons appeared at 3.7 and 1.2 ppm. We noted the monomodal profile of the GPC trace confirming the absence of side reaction and the integrity of the end-group (Fig. S1).

### 3.2. Coatings characterisation

The surface topography has an influence on both the wetting ability, the colonisation and adhesion of bacteria. Smooth silicone surface is known to limit bacterial adhesion [27], so coatings surfaces were observed by microscopy. Another important parameter for amphiphilic coatings is the hydrophilic character of the surface [18], so it was measured by contact angle as this can indicate the presence of additive at the surface. Finally, to be efficient, the amphiphilic coating has to be homogeneous without macrophase. One of the key parameters for silicone fouling release is the elastic modulus [28]. Formation of domain can generate a loss of the silicone physical properties. Coating composition was determined by confocal Raman microscopy to evaluate polymer distribution.

The additive amount chosen was 10% in weight. Recent research has indeed shown that this amount of additives in an amphiphilic PEG-silicone coating resulted in a drastic reduction of bacteria, diatom and mixed biofilm formation [29]. The coatings prepared for this study were dried during 4 days before any use, to remove all the solvent used and to have the highest crosslinking rate. The thickness of the dry coatings was approximately 200 µm.

#### 3.2.1. Surface topography

Fouling release coatings using silicone are used to prevent bioadhesion due to their low roughness. This parameter allows a low colonisation and promotes the release of fouling [30]. Roughness of the coating surface could be caused by the crosslinking reaction or an inhomogeneity of the coating components. Pictures and results obtained for the silicone reference showed a smooth surface (Fig. 4). The crosslinking system and the catalyst-solvent combination-proportion seemed efficient.

From the SEM images, we observed that the addition of PEG and POx led to a modification of the surface topography (Fig. 4). The solidification of the additives at the surface during the drying process, could explain such modification. Indeed, PEG and POx of 2000 g.mol$^{-1}$ are solid at room temperature. A recent study has shown the formation of PEG-silicone film without roughness modification when a lower molecular weight of PEG (liquid a room temperature) is used [31]. Nevertheless, microscope pictures obtained by SEM showed an uniform profile over the whole surface area.

From the profilometry images, we clearly observe that the roughness depends on the hydrophilic polymers additives (Fig. 4). The averaged roughness (Sq) for POx-PDMS is about 3 µm while the roughness found for PEG-PDMS is similar to the neat PDMS (Sq 0.7 µm). Accordingly, these results show that the embedding of the additives during the crosslinking reaction and drying was better for the PEG additive. The thermal properties, in particular the glass transition, could explain the difference between the additives. Poly(2methyl-2-oxazoline) has a glass transition temperature higher than the room temperature (80 °C) unlike PEG (–20 °C) [32,33]. Therefore, the polymer chains mobility was lower for the POx during the preparation process and promoted the surface roughness.

#### 3.2.2. Surface properties

Addition of hydrophilic additives in silicone coating increased lubricity and decreased bioadhesion [15]. To be efficient, hydrophilic polymer needs to diffuse through the coating and reach its surface. However, the presence of a crosslinking group on the additives limits the diffusion in the coating and only polymer chains close to the surface can reach it. However, the crosslinking group was required to limit the release into the environment and to increase the lifespan of the coating.

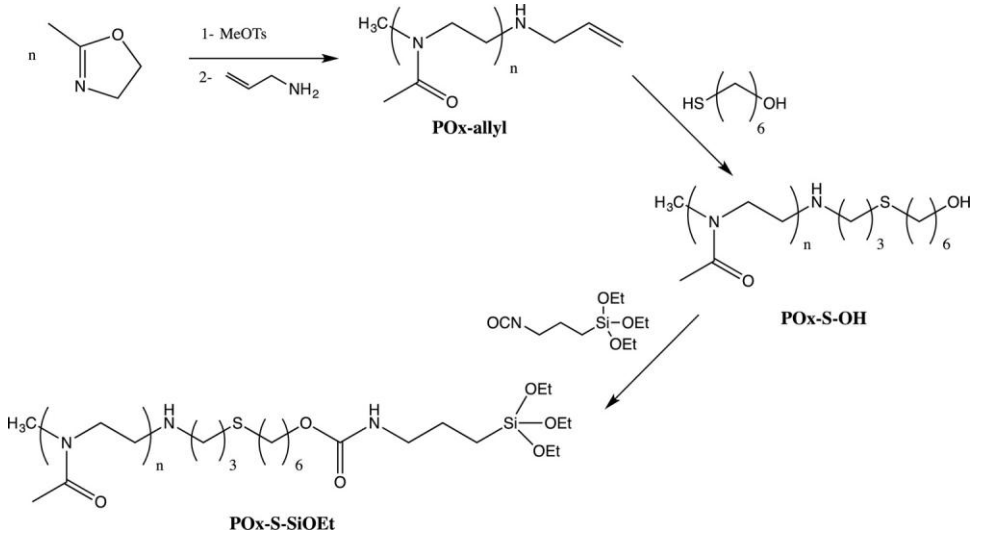


**Fig. 2.** POx functionalization with a triethoxysilane end-group.

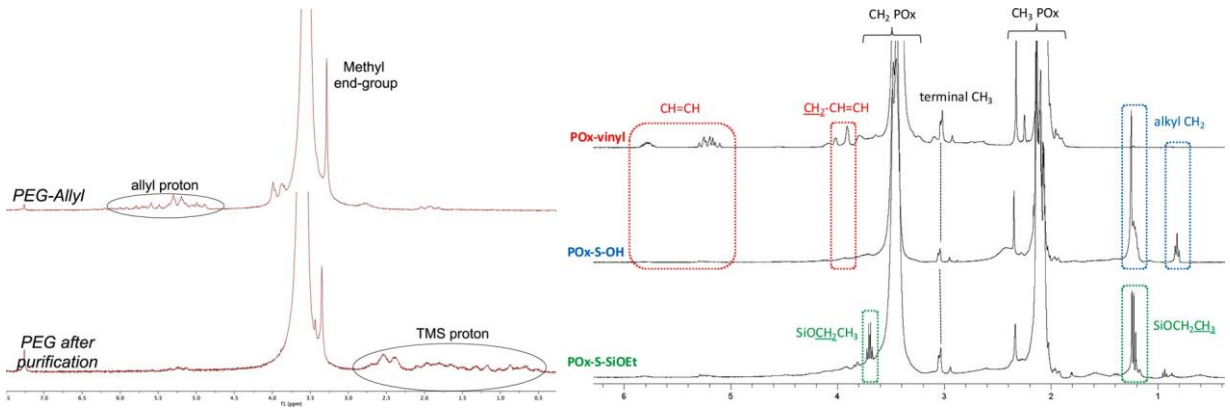


**Fig. 3.** $^{1}$H NMR spectra of PEG additives before and after thiol-ene reaction (Spinsolve 60 MHz) and $^{1}$H NMR spectrum of POx modifications (300 MHz).

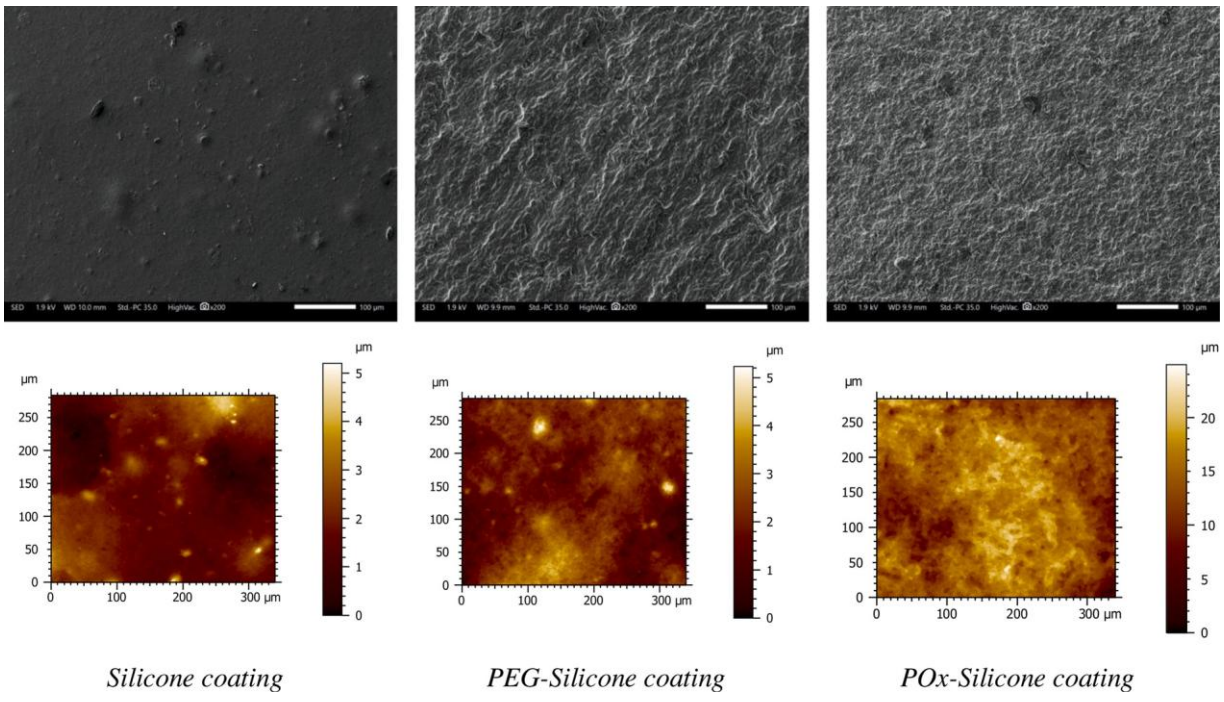


**Fig. 4.** Topography of the modified PDMS samples observed by SEM (x 200 magnification) and optical profilometry.

The size of the additives and the compatibility between the silicone and the additive could be determinant in its mobility to reach the surface as well [34]. PEG and POx additives have the same molecular weight to be compared.

The results obtained for contact angle kinetics were shown in the Table 1. The neat PDMS coating used as reference has a hydrophobic surface with a static contact angle of 110° and during the first 15 s no change of the angle was observed. The fillers present in the commercial coatings have no influence on the hydrophobicity in presence of water.

**Table 1**
Results of the contact angle kinetics on the coating surfaces with a water droplet of 2 µL (standard deviation of 0,2°).

| | Contact angle $t$ = 0 | Decrease of angle in 15 s | Decrease of angle 15–60 s |
|---|---|---|---|
| Silicone | 110° | 0° | 6° |
| PEG-silicone | 110° | 10° | 6° |
| POx-silicone | 118° | 6° | 6° |

After 15 s, the decrease of the angle was due to water evaporation [35, 36]. Indeed, a decrease of the droplet volume was also observed (Fig. S2). Coatings containing the hydrophilic additives showed a decrease of the contact angle before water evaporation. The presence of additives onto the surface can explain these results. After 15 s, the same evolution as for the PDMS reference was observed. Only water evaporation occurred. Two differences between the PEG-silicone and the POx-silicone coatings were observed. The POx-silicone had a superior contact angle to the silicone coating at the beginning (respectively 118° and 110°). Some interactions between fillers and the amine of the poly (oxazoline) could explain the increase of hydrophobicity. Experiments made with a neat silicone gave the same result for both coating (data not shown). No difference was observed for the PEG-silicone coating. Moreover, the decrease of contact angle during 15 s was lower for the POx-silicone coating. As observed previously for the surface topography, compatibility between the PEG and the commercial PDMS seemed better.

### 3.2.3. *Coating composition*

Studying the overall homogeneity of the composite films and the

interactions between the components are essential to understand the changes in surface properties [34]. Aggregates formation can modify antibacterial efficiency and promote bioadhesion by impairing physico-chemical properties. Pictures and spectra obtained by confocal Raman microscopy are shown in the Fig. 5. Vibrational information obtained from a Raman spectrum is rich in content about both the chemical and morphological structure of polymers [37,38] and antimicrobial composite materials [39]. The small diameter of the laser beam allows fine spatial resolution. Consequently, Raman confocal imaging makes it easy to check the quality of a sample and can provide a spatial distribution of the chemical composition [40].

In the wavenumber range of 1200−2000 $cm^{-1}$, the Raman spectrum of PEG is characterized by well-resolved bands at 1482 $cm^{-1}$ attributed to the deformation of $CH_2$ scissoring vibration with a contribution of backbone (OCC——) deformation, and two bands located at 1279 and 1233 $cm^{-1}$ assigned to the gauche mode vibration and the trans mode vibration of the CC— group, respectively [41,42]. The Raman spectrum of POx is characterized mainly by a broad band centred at 1635 $cm^{-1}$ attributed to the CN— stretching vibrations and broad bands in the 1400-1500 $cm^{-1}$ range (with peaks located at 1483, 1467 and 1439 $cm^{-1}$ assigned to the in plane bending of the $CH_2$ groups [43].

WITec specific True Component Analysis (TCA) allowed us to identify pixels of a map with similar spectra and provide these spectral characteristics (i.e., similar to chemical response) in an intensity distribution image. A significant difference was observed during these investigations between both additives. PEG distribution was more homogeneous and PEG seems to have more affinity with the PDMS than POx. Indeed, from the surface analysis, the formation of macrodomains whose size varies from 2 to 6 µm in diameter (blue in Fig. 5.b) was observed for the POx-PDMS. PEG distribution on the surface (green in Fig. 5.a) was more dispersed. Indepth analysis were carried out on the same samples. For improve clarity, all Raman spectra were shifted in intensity. Along the transverse section, the Raman spectra of the PEG-PDMS films show the presence of the main vibrational bands of the PEG. As the band intensities relative to the PEG are similar, it can be concluded that the PEG is well dispersed into the film. For the POx-PDMS sample, the band intensities of POx changed depending on depth, revealing a random distribution of the component into the film. These results confirmed the better compatibility between PEG and silicone mentioned previously.

To conclude, the compatibility between silicone and poly(oxazoline) was lower than with the PEG. The introduction of POx altered the quality of the silicone coating. The increase of the roughness and the formation of macrophase should impact fouling release efficiency.

### 3.3. Anti-bacterial properties

#### 3.3.1. Adhesion assay

Before the adhesion tests, the toxicity of coatings was verified. The growth of bacteria was evaluated by $OD_{600nm}$ measurement.

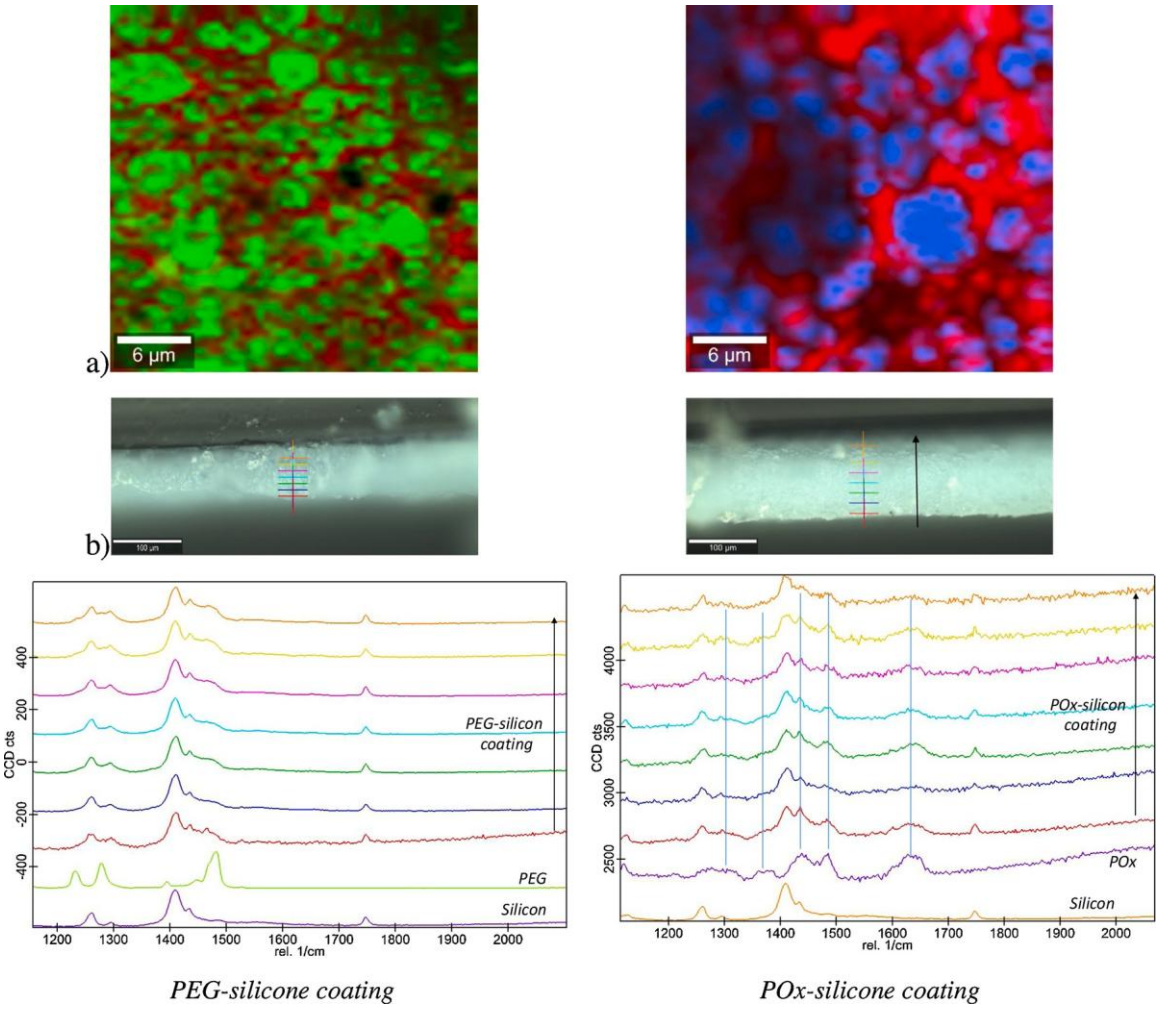


**Fig. 5.** Additives distribution determined by confocal Raman microscopy. a) Silicone (red), PEG (green) and POx (blue) on the surface of the coatings. b) Raman spectra along the transverse section of the PEG-silicone and POx-silicone films. (For interpretation of the references to color in this figure legend, the reader is referred to the web version of this article.).

*P. aeruginosa* and *S. aureus* were grown as in a standard condition, on PDMS, PEG-silicone or POx-silicone. Concerning *Pseudoalteromonas* 5M6, compared to a control condition, the growth was similar for both conditions PDMS and PEG-silicone. However, POx-silicone coating showed bacteriostatic effect (Data not shown). Many studies have already shown that polymers did not have any toxic effect on bacteria (*E. coli, S; aureus, S. epidermidis, P. aeruginosa*) and human cells [44–46].

In a second experiment, the ability of bacteria to adhere to different coatings and their adhesion strength on these surfaces were evaluated. After the injection of bacteria into flow cell, the step of adhesion lasted 2 h. Peristaltic pump was adjusted at 0.25 mL.min$^{-1}$; 6.16 mPa, and the planktonic cells were harvested for one hour, spread on plate agar and colonies were counted. For the three strains, the concentration of bacteria harvested was between $10^5$ and $10^6$ ufc.mL$^{-1}$, and this was observed for each surface. Whatever the coating, there is no difference in the adhesion of microorganisms. Then the flow rate was adjusted at 2.95 mL.min$^{-1}$ to mimic the shear stress in a catheter. Bacteria were harvested for 30 min and were spread on an agar plate and counted after incubation. Results obtained for *P. aeruginosa* showed no difference between both PDMS and PEG-silicone (Fig. 6). However, the concentration of bacteria release from POx-silicone ($1.43 \times 10^3$ ufc.mL$^{-1}$) surfaces was significantly higher than from the PDMS surface ($3.58 \times 10^2$ ufc.mL$^{-1}$). Bacteria seemed more strongly attached to PDMS coating.

Concerning *S. aureus*, results were very interesting. In fact, after 30 min of flow, no bacteria were counted in the PDMS condition compared to the PEG-silicone or POx-silicone conditions for which $1.2 \times 10^3$ ufc.mL$^{-1}$ and $2.5 \times 10^2$ ufc.mL$^{-1}$ were respectively harvested.

Finally, a significant difference was observed between concentration of *Pseudoalteromonas* 5M6 released from PDMS and PEG-silicone surfaces. On average, $2.58 \times 10^3$ ufc.mL$^{-1}$ were estimated for the PDMS surface, against $4.59 \times 10^4$ ufc.mL$^{-1}$ harvested from the PEG-silicone surface. No difference was observed between PDMS and POx-silicone. Few studies have ever demonstrated the microorganisms' strength of adhesion on these coatings. However, several papers described the adhesion and anti-fouling properties of PEG and POx coatings [47–49], mainly in minimal culture condition [50]. Our results seem agree with previous observations by Cavallaro and coworkers. Who have shown that bacteria were able to attach on coatings made of POx, but that the strength of adhesion was very weak. Both cells adhered and biofilms came off surfaces during simple washing [51].

### 3.3.2. Scanning electron microscopy

In view of the results obtained for *S. aureus* strain, we decided to perform scanning electronic microscopy observations. Fig. 7 shows the SEM microphotographs of *S. aureus* adhered on PDMS, PEG-silicone and POx-silicone. This experiment allowed, first, the characterization of topography of the different coatings, and the visualization of bacterial adhesion.

As observed previously, the three surfaces did not have the same topography. In fact, PDMS seemed to be more homogenous with a smoother surface. PEG-silicone and POx-silicone surfaces seemed rougher and more heterogeneous. PEG and POx seemed to be dispersed in PDMS matrix, but the dispersion was not uniform, probably responsible for different roughness degrees. Cavities appeared on the PEG-silicone surfaces.

On PDMS coating, bacteria formed clusters and their distribution was homogeneous, bacteria also formed a single layer. Looking closer, we could see that bacteria were sinked into soft part of PDMS coating. On the two other coatings, bacteria adhered to the entire surface. In addition, these bacteria began to produce matrices and filaments (Fig. 7; white arrow) and they formed clusters in several layers.

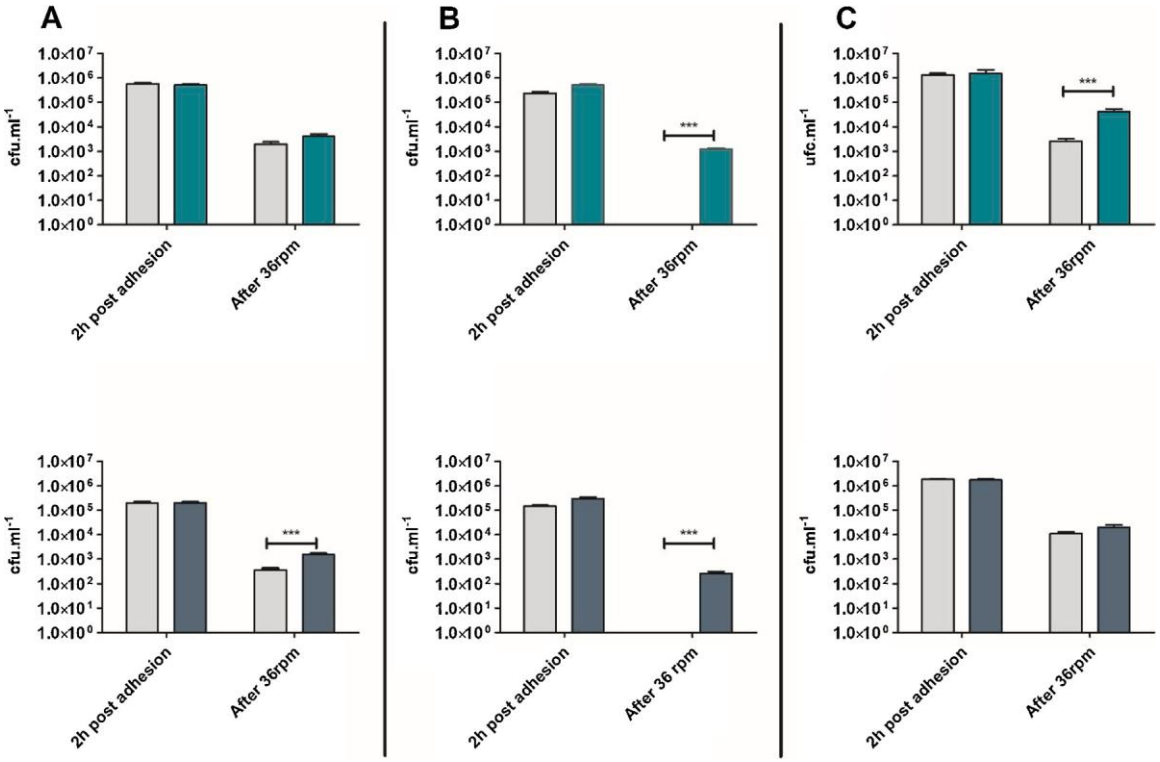


**Fig. 6.** Adhesion test on PDMS (grey bars) vs PEG-silicone (green bars, graph on the top) and POx-silicone (blue bars, graph on the bottom). *P. aeruginosa* (A), *S. aureus* (B) and *Pseudoalteromonas* 5M6 (C) were tested for their ability to adhered on the different surfaces. After adhesion, planktonic cells were harvested, spread and counted on plate agar (2 h post adhesion). A 36 rpm flow was applied for 30 min to unhook bacteria which were not solidly adhered. Cells were harvested, spread and counting on plate agar (After 36 rpm). Results are expressed in cfu.ml$^{-1}$. Data represent the mean +/- standard error of the mean (SEM) from triplicates of five independent experiments (*** $p$-value < 0.001 Mann Whitney $U$ test). (For interpretation of the references to color in this figure legend, the reader is referred to the web version of this article.)

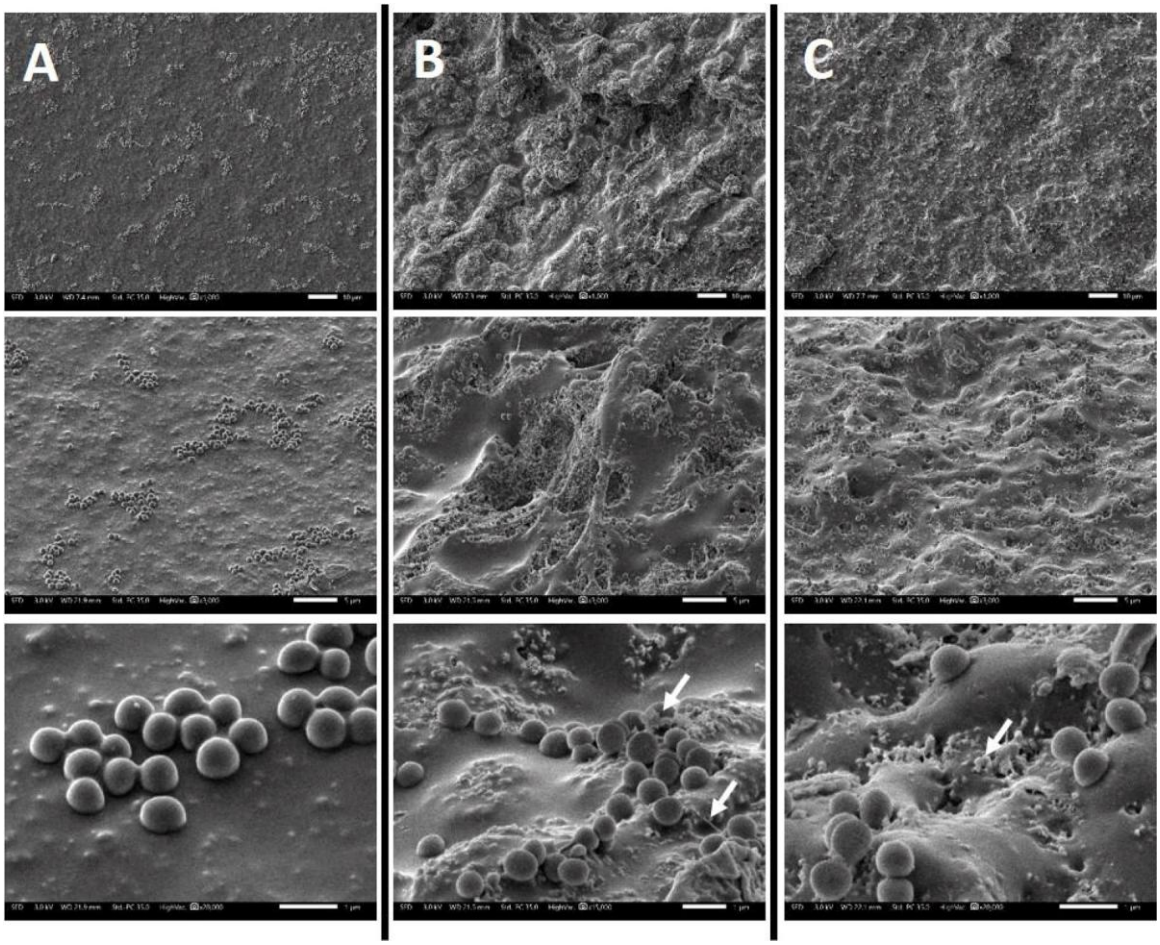


**Fig. 7.** Adhesion of *S. aureus* on PDMS (A), PEG-silicone (B) and POx-silicone (C), observed by scanning electron microscopy. From top to bottom, scale bars correspond to 10 µm, 5 µm and 1 µm.

Correlated with results of the adhesion assay, these observations suggest that bacteria adhered more strongly on PDMS coating than on the two others which were less homogeneous. When flow was increased, bacteria stayed trapped into PDMS coating. On the other hand, on the both PEG-silicone and POx-silicone coatings, matrix production had started, and bacteria were trapped, forming micro-colonies. And the flow took off part of these consortia. This hypothesis could explain the results of our adhesion assay.

*S. aureus* expressed many surfaces proteins like ClfA and ClfB (Mc Devitt et al.). They favoured interaction between cells. Other proteins were produced (Fg, SraP, Ebh ClfA, SasG), more later, and allowed biofilms development [52,53]. These proteins seemed expressed by *S. aureus*. Moreover, after adhesion step, *S. aureus* started to produce a matrix made of polysaccharides named polysaccharides intracellular adhesion (PIA). They are polymeric N-acethyl glucosamine (PNAG) They were essential for the biofilm integrity [54]. Matrix was also made of extracellular DNA (eDNA), released after autolyzed cells. eDNA had an important part during cell attachment [55]. It was possible, that the filaments observed in Fig. 7 were eDNA.

## 4. Conclusion

In this study, the interest of poly(oxazoline) as additives in amphiphilic fouling release coating was showed. POx additive had a similar anti-bacterial property than PEG. The incorporation of POx did not decrease bacterial colonisation compared to PDMS coating. However, as already observed with PEG, adhesion strength was reduced and the fouling release ability of the coating increased. However, POx-silicone coating needs to be improved. The compatibility between POx and PDMS is lower than between PEG and PDMS. It should have an impact on the viscoelasticity of the coating. In addition, POx incorporation increases the surface roughness of the coating. Viscoelasticity and surface roughness are also key parameters for the PDMS based fouling release coating efficiency.

## Author's contribution

- All authors have participated in (a) conception and design, or analysis and interpretation of the data; (b) drafting the article or revising it critically for important intellectual content; and (c) approval of the final version.
- This manuscript has not been submitted to, nor is under review at, another journal or other publishing venue.
- The authors have no affiliation with any organization with a direct or indirect financial interest in the subject matter discussed in the manuscript

## CRediT authorship contribution statement

**Émilie Portier:** Conceptualization, Methodology, Investigation, Resources, Writing - review & editing. **Fabrice Azemar:** Conceptualization, Methodology, Investigation, Resources, Writing - review & editing, Project administration. **Belkacem Tarek Benkhaled:** Methodology, Investigation. **Jean-François Bardeau:** Methodology, Investigation, Resources, Writing - review & editing. **Fabienne Faÿ:** Supervision. **Karine Réhel:** Funding acquisition, Writing - review & editing. **Vincent**

**Lapinte:** Funding acquisition, Writing - review & editing. **Isabelle Linossier:** Funding acquisition, Project administration.

## Declaration of Competing Interest

The authors report no declarations of interest.

## Acknowledgements

This work was supported by ANR SAFER15-LCV4-0006. This manuscript is a tribute to the 50 year anniversary of the French Polymer Group (Groupe Français des Polymères - GFP).

## Appendix A. Supplementary data

Supplementary material related to this article can be found, in the online version, at doi:https://doi.org/10.1016/j.porgcoat.2020.106116.

## References

[1] J.W. Costerton, Bacterial biofilms: a common cause of persistent infections, Science 284 (5418) (1999) 1318–1322, https://doi.org/10.1126/science.284.5418.1318.
[2] D.G. Allison, B. Ruiz, C. SanJose, A. Jaspe, P. Gilbert, Extracellular products as mediators of the formation and detachment of *Pseudomonas fluorescens* biofilms, FEMS Microbiol. Lett. 167 (2) (1998) 179–184, https://doi.org/10.1111/j.1574-6968.1998.tb13225.x.
[3] P.A. Marshall, Response of microbial adhesives and biofilm matrix polymers to chemical treatments as determined by interference reflection microscopy and light section microscopyt, Appl. Environ. Microbiol. 55 (1989) 5.
[4] P.S. Stewart, Mechanisms of antibiotic resistance in bacterial biofilms, Int. J. Med. Microbiol. 292 (2) (2002) 107–113, https://doi.org/10.1078/1438-4221-00196.
[5] L.R. Mulcahy, J.L. Burns, S. Lory, K. Lewis, Emergence of Pseudomonas aeruginosa strains producing high levels of persister cells in patients with cystic fibrosis, J. Bacteriol. 192 (23) (2010) 6191–6199, https://doi.org/10.1128/JB.01651-09.
[6] Preston, B. L.; Shackelford, J. Multiple Stressor Effects on Benthic Biodiversity of Chesapeake Bay: Implications for Ecological Risk Assessment. 15.
[7] D. Meseguer Yebra, S. Kiil, C.E. Weinell, K. Dam-Johansen, Presence and effects of marine microbial biofilms on biocide-based antifouling paints, Biofouling 22 (1) (2006) 33–41, https://doi.org/10.1080/08927010500519097.
[8] U. Eduok, O. Faye, J. Szpunar, Recent developments and applications of protective silicone coatings: a review of PDMS functional materials, Prog. Org. Coat. 111 (2017) 124–163, https://doi.org/10.1016/j.porgcoat.2017.05.012.
[9] J. Stein, K. Truby, C.D. Wood, J. Stein, M. Gardner, G. Swain, C. Kavanagh, B. Kovach, M. Schultz, D. Wiebe, E. Holm, J. Montemarano, D. Wendt, C. Smith, Meyer, A. Silicone foul release coatings: effect of the interaction of oil and coating functionalities on the magnitude of macrofouling attachment strengths, Biofouling 19 (Sup1) (2003) 71–82, https://doi.org/10.1080/0892701031000089525.
[10] K. Truby, C. Wood, J. Stein, J. Cella, J. Carpenter, C. Kavanagh, G. Swain, D. Wiebe, D. Lapota, A. Meyer, E. Holm, D. Wendt, C. Smith, J. Montemarano, Evaluation of the performance enhancement of silicone biofouling-release coatings by oil incorporation, Biofouling 15 (1–3) (2000) 141–150, https://doi.org/10.1080/08927010009386305.
[11] A. Meyer, R. Baier, C.D. Wood, J. Stein, K. Truby, E. Holm, J. Montemarano, C. Kavanagh, B. Nedved, C. Smith, G. Swain, D. Wiebe, Contact angle anomalies indicate that surface-active eluates from silicone coatings inhibit the adhesive mechanisms of fouling organisms, Biofouling 22 (6) (2006) 411–423, https://doi.org/10.1080/08927010601025473.
[12] M. Nendza, Hazard assessment of silicone oils (Polydimethylsiloxanes, PDMS) used in antifouling-/Foul-Release-Products in the marine environment, Mar. Pollut. Bull. 54 (8) (2007) 1190–1196, https://doi.org/10.1016/j.marpolbul.2007.04.009.
[13] J. Karlsson, B. Eklund, New biocide-free anti-fouling paints are toxic, Mar. Pollut. Bull. 49 (5) (2004) 456–464, https://doi.org/10.1016/j.marpolbul.2004.02.034.
[14] N. Filip, A. Pustam, V. Ells, K.M.T. Grosicki, J. Yang, I. Oguejiofor, C.D. Bishop, M. E. DeMont, T. Smith-Palmer, R.C. Wyeth, Fouling-release and chemical activity effects of a siloxane-based material on tunicates, Mar. Environ. Res. 116 (2016) 41–50, https://doi.org/10.1016/j.marenvres.2016.02.015.
[15] T. Røn, I. Javakhishvili, S. Hvilsted, K. Jankova, S. Lee, Ultralow friction with hydrophilic polymer brushes in water as segregated from silicone matrix, Adv. Mater. Interfaces 3 (2) (2016) 1500472, https://doi.org/10.1002/admi.201500472.
[16] Z. Wu, K. Hjort, Surface modification of PDMS by gradient-induced migration of embedded pluronic, Lab Chip 9 (11) (2009) 1500–1503, https://doi.org/10.1039/b901651a.
[17] H. Fabre, D. Mercier, A. Galtayries, D. Portet, N. Delorme, J.-F. Bardeau, Impact of hydrophilic and hydrophobic functionalization of flat $TiO_2$/Ti surfaces on proteins adsorption, Appl. Surf. Sci. 432 (2018) 15–21, https://doi.org/10.1016/j.apsusc.2017.08.138.
[18] A. Camós Noguer, S.M. Olsen, S. Hvilsted, S. Kiil, Diffusion of surface-active amphiphiles in silicone-based fouling-release coatings, Prog. Org. Coat. 106 (2017) 77–86, https://doi.org/10.1016/j.porgcoat.2017.02.014.
[19] M. Grube, M.N. Leiske, U.S. Schubert, I. Nischang, POx as an alternative to PEG? A hydrodynamic and light scattering study, Macromolecules 51 (5) (2018) 1905–1916, https://doi.org/10.1021/acs.macromol.7b02665.
[20] T.X. Viegas, M.D. Bentley, J.M. Harris, Z. Fang, K. Yoon, B. Dizman, R. Weimer, A. Mero, G. Pasut, F.M. Veronese, Polyoxazoline: chemistry, properties, and applications in drug delivery, Bioconjug. Chem. 22 (5) (2011) 976–986, https://doi.org/10.1021/bc200049d.
[21] L. Simon, M. Vincent, S. Le Saux, V. Lapinte, N. Marcotte, M. Morille, C. Dorandeu, J.M. Devoisselle, S. Bégu, Polyoxazolines based mixed Micelles as PEG free formulations for an effective quercetin antioxidant topical delivery, Int. J. Pharm. 570 (2019) 118516, https://doi.org/10.1016/j.ijpharm.2019.118516.
[22] B. Guillerm, S. Monge, V. Lapinte, J.-J. Robin, How to modulate the chemical structure of polyoxazolines by appropriate functionalization, Macromol. Rapid Commun. 33 (19) (2012) 1600–1612, https://doi.org/10.1002/marc.201200266.
[23] M. Glassner, M. Vergaelen, R. Hoogenboom, Poly(2-Oxazoline)s: a comprehensive overview of polymer structures and their physical properties, Polym. Int. 67 (1) (2018) 32–45, https://doi.org/10.1002/pi.5457.
[24] J. Ulbricht, R. Jordan, R. Luxenhofer, On the biodegradability of polyethylene glycol, polypeptoids and poly(2-Oxazoline)s, Biomaterials 35 (17) (2014) 4848–4861, https://doi.org/10.1016/j.biomaterials.2014.02.029.
[25] Q. Yang, S.K. Lai, Anti-PEG immunity: emergence, characteristics, and unaddressed questions, WIREs Nanomed. Nanobiotechnol. 7 (5) (2015) 655–677, https://doi.org/10.1002/wnan.1339.
[26] D.D. Perrin, W.L.F. Armarego, D.R. Perrin, Purification of Laboratory Chemicals, second ed., Pergamon Press: Oxford, New York, 1980.
[27] Dantas, L. C. de M.; Silva-Neto, J. P. da; Dantas, T. S.; Naves, L. Z.; das Neves, F. D.; da Mota, A. S. Bacterial Adhesion and Surface Roughness for Different Clinical Techniques for Acrylic Polymethyl Methacrylate https://www.hindawi.com/journals/ijd/2016/8685796/ (Accessed Apr 28, 2020). https://doi.org/10.1155/2016/8685796.
[28] Robert F. Brady, R. F. B, I.L. Singer, Mechanical factors favoring release from fouling release coatings, Biofouling 15 (1–3) (2000) 73–81, https://doi.org/10.1080/08927010009386299.
[29] F. Faÿ, M.L. Hawkins, K. Réhel, M.A. Grunlan, I. Linossier, Non-toxic, anti-fouling silicones with variable PEO–silane amphiphile content, Int. J. Green Nanotechnol. Mater. Sci. Eng. 4 (2) (2016) 53–62, https://doi.org/10.1680/jgrma.16.00003.
[30] M. Lejars, A. Margaillan, C. Bressy, Fouling release coatings: a nontoxic alternative to biocidal antifouling coatings, Chem. Rev. 112 (8) (2012) 4347–4390, https://doi.org/10.1021/cr200350v.
[31] R. Majumdar, K.S. Alexander, A.T. Riga, Physical characterization of polyethylene glycols by thermal analytical technique and the effect of humidity and molecular weight, Pharmazie 65 (5) (2010) 343–347.
[32] E. Rettler, J.M. F.-J.; Kranenburg, H.M.L. Lambermont-Thijs, R. Hoogenboom, U. S. Schubert, Thermal, mechanical, and surface properties of poly(2-N-Alkyl-2-Oxazoline)s, Macromol. Chem. Phys. 211 (22) (2010) 2443–2448, https://doi.org/10.1002/macp.201000338.
[33] J.A. Faucher, J.V. Koleske, E.R. Santee, J.J. Stratta, C.W. Wilson, Glass transitions of ethylene oxide polymers, J. Appl. Phys. 37 (11) (1966) 3962–3964, https://doi.org/10.1063/1.1707961.
[34] G. Gillet, F. Azemar, F. Faÿ, K. Réhel, I. Linossier, Non-leachable hydrophilic additives for amphiphilic coatings, Polymers 10 (4) (2018) 445, https://doi.org/10.3390/polym10040445.
[35] S.S. Sadhal, M.S. Plesset, Effect of solid properties and contact angle in dropwise condensation and evaporation, J. Heat Transf. 101 (1) (1979) 48–54, https://doi.org/10.1115/1.3450934.
[36] S. Chandra, M. di Marzo, Y.M. Qiao, P. Tartarini, Effect of liquid-solid contact angle on droplet evaporation, Fire Saf. J. 27 (2) (1996) 141–158, https://doi.org/10.1016/S0379-7112(96)00040-9.
[37] G. Vignaud, J.-F. Bardeau, A. Gibaud, Y. Grohens, Multiple glass-transition temperatures in thin supported films of isotactic PMMA as revealed by enhanced raman scattering, Langmuir 21 (19) (2005) 8601–8604, https://doi.org/10.1021/la050898b.
[38] A.A. Pud, K.Y. Fatyeyeva, J.-F. Bardeau, S.P. Rogalsky, M. Tabellout, G. S. Shapoval, Polyamide-12/Polyaniline layered composite films: specificity of the formation and Raman spectroscopy investigation, J. Macromol. Sci. Part A 44 (2) (2007) 183–192, https://doi.org/10.1080/10601320601031358.
[39] S. Rogalsky, J.-F. Bardeau, H. Wu, L. Lyoshina, O. Bulko, O. Tarasyuk, S. Makhno, T. Cherniavska, Y. Kyselov, J.H. Koo, Structural, thermal and antibacterial properties of polyamide 11/polymeric biocide polyhexamethylene guanidine dodecylbenzenesulfonate composites, J. Mater. Sci. 51 (16) (2016) 7716–7730, https://doi.org/10.1007/s10853-016-0054-x.
[40] G. Giridhar, R.R.K.N. Manepalli, G. Apparao, Chapter 7 - confocal Raman spectroscopy, in: S. Thomas, R. Thomas, A.K. Zachariah, R.K. Mishra (Eds.), Spectroscopic Methods for Nanomaterials Characterization, Micro and Nano Technologies; Elsevier, 2017, pp. 141–161, https://doi.org/10.1016/B978-0-323-46140-5.00007-8.
[41] M. El Hadri, A. Achahbar, J. El Khamkhami, B. Khelifa, V. Faivre, T.T. Cong, F. Bougrioua, S. Bresson, Raman spectroscopy investigation of mono- and diacyl-polyoxyethylene glycols, Vib. Spectrosc. 64 (2013) 78–88, https://doi.org/10.1016/j.vibspec.2012.11.006.
[42] A.Z. Samuel, S. Umapathy, Energy funneling and macromolecular conformational dynamics: a 2D Raman correlation study of PEG melting, Polym. J. 46 (6) (2014) 330–336, https://doi.org/10.1038/pj.2014.10.

[43] J.R. Durig, S. Riethmiller, Y.S. Li, Spectra and structure of small ring compounds. XXXI microwave, Raman and infrared spectra, conformation, dipole moment, and quadrupole coupling constants of 2-oxazoline, J. Chem. Phys. 61 (1) (1974) 253–262, https://doi.org/10.1063/1.1681630.
[44] R. Hoogenboom, Poly(2-Oxazoline)s: a polymer class with numerous potential applications, Angew. Chem. Int. Ed. 48 (43) (2009) 7978–7994, https://doi.org/10.1002/anie.200901607.
[45] T. Vermonden, R. Censi, W.E. Hennink, Hydrogels for protein delivery, Chem. Rev. 112 (5) (2012) 2853–2888, https://doi.org/10.1021/cr200157d.
[46] H. Zhang, M. Chiao, Anti-fouling coatings of poly(Dimethylsiloxane) devices for biological and biomedical applications, J. Med. Biol. Eng. 35 (2) (2015) 143–155, https://doi.org/10.1007/s40846-015-0029-4.
[47] C. Zhou, Y. Wu, K.R.V. Thappeta, J.T.L. Subramanian, D. Pranantyo, E.-T. Kang, H. Duan, K. Kline, M.B. Chan-Park, In vivo anti-biofilm and anti-bacterial non-leachable coating thermally polymerized on cylindrical catheter, ACS Appl. Mater. Interfaces 9 (41) (2017) 36269–36280, https://doi.org/10.1021/acsami.7b07053.
[48] B. Pidhatika, M. Rodenstein, Y. Chen, E. Rakhmatullina, A. Mühlebach, C. Acikgöz, M. Textor, R. Konradi, Comparative stability studies of poly(2-Methyl-2-Oxazoline) and poly(Ethylene glycol) brush coatings, Biointerphases 7 (1) (2012) 1, https://doi.org/10.1007/s13758-011-0001-y.
[49] L. Tauhardt, K. Kempe, M. Gottschaldt, U.S. Schubert, Poly(2-Oxazoline) functionalized surfaces: from modification to application, Chem. Soc. Rev. 42 (20) (2013) 7998–8011, https://doi.org/10.1039/C3CS60161G.
[50] I.C. Saldarriaga Fernández, H.C. van der Mei, M.J. Lochhead, D.W. Grainger, H. J. Busscher, The inhibition of the adhesion of clinically isolated bacterial strains on multi-component cross-linked poly(Ethylene glycol)-Based polymer coatings, Biomaterials 28 (28) (2007) 4105–4112, https://doi.org/10.1016/j.biomaterials.2007.05.023.
[51] A.A. Cavallaro, M.N. Macgregor-Ramiasa, K. Vasilev, Antibiofouling properties of plasma-deposited oxazoline-based thin films, ACS Appl. Mater. Interfaces 8 (10) (2016) 6354–6362, https://doi.org/10.1021/acsami.6b00330.
[52] J.A. Geoghegan, R.M. Corrigan, D.T. Gruszka, P. Speziale, J.P. O'Gara, J.R. Potts, T.J. Foster, Role of surface protein SasG in biofilm formation by Staphylococcus aureus, J. Bacteriol. 192 (21) (2010) 5663–5673, https://doi.org/10.1128/JB.00628-10.
[53] R.M. Corrigan, D. Rigby, P. Handley, T.J. Foster, The role of Staphylococcus aureus surface protein SasG in adherence and biofilm formation, Microbiology 153 (8) (2007) 2435–2446, https://doi.org/10.1099/mic.0.2007/006676-0.
[54] D. Mack, W. Fischer, A. Krokotsch, K. Leopold, R. Hartmann, H. Egge, R. Laufs, The intercellular adhesin involved in biofilm accumulation of Staphylococcus epidermidis is a linear Beta-1,6-Linked glucosaminoglycan: purification and structural analysis, J. Bacteriol. 178 (1) (1996) 175–183, https://doi.org/10.1128/jb.178.1.175-183.1996.
[55] K.C. Rice, E.E. Mann, J.L. Endres, E.C. Weiss, J.E. Cassat, M.S. Smeltzer, K. W. Bayles, The CidA murein hydrolase regulator contributes to DNA release and biofilm development in Staphylococcus aureus, Proc. Natl. Acad. Sci. 104 (19) (2007) 8113–8118, https://doi.org/10.1073/pnas.0610226104.